

# Temperature dependence of the degree of compatibility in SBR–NBR blends by ultrasonic attenuation measurements: influence of unsaturated polyester additive

M.H. Youssef

*Department of Physics, Faculty of Science, Cairo University, Giza 12612, Egypt*

Received 19 April 2001; accepted 27 July 2001

## Abstract

The dependence of ultrasonic attenuation coefficient on temperature is measured for styrene–butadiene rubber (SBR), acrylonitrile–butadiene rubber (NBR) and their blends (SBR/NBR = 25/75, 50/50, 75/25 by wt) in the temperature range from 240 to 342 K at ultrasonic frequency of 5 MHz. The obtained ultrasonic relaxation peaks due to glass–rubber transition were used to investigate the degree of compatibility (DC) in the blends as well as its variation with temperature. The addition of 10 phr of unsaturated polyester resin (based on *p*-carboxy phthalanilic acid and maleic anhydride with ethylene glycol) to the blend showed improvement of DC in certain temperature ranges and deterioration of DC in other temperature ranges. © 2001 Elsevier Science Ltd. All rights reserved.

*Keywords:* SBR–NBR blends; Unsaturated polyester; Ultrasonic attenuation

## 1. Introduction

The physical blending of two polymers gives a new product whose physical and mechanical properties are usually different from those of the individual components. The degree of compatibility (DC) of the two components plays an essential role in the applicability of the final product in many industrial fields. Two polymeric components are compatible if the mixing takes place at the molecular level. From the thermodynamic point of view, complete compatibility is not a common feature of polymers due to the entropy gain by mixing different kinds of long chains. However, a certain degree of mixing may take place to produce a semi-compatible blend.

Many experimental techniques are widely used for determining DC. These are electron microscopy, optical clarity, differential scanning calorimetry (DSC), differential thermal analysis (DTA) and dielectric permittivity. Two extremely accurate techniques are also used for investigation of DC, namely, dynamic mechanical thermal analysis (DMTA) [1–3] and ultrasonic (US) velocity and attenuation measurements [4–11]. In a recent work by Youssef et al. [12], 5 phr of unsaturated polyester (UPE) resin was added to styrene–butadiene rubber (SBR) and acrylonitrile–

butadiene rubber (NBR). The US dynamic glass transition temperatures  $T_g$  of the two polymers were found to approach each other by addition of UPE. This encouraged the same co-workers to investigate the effect of UPE additive on the compatibility of SBR and NBR in their physical blends [13]. The study was carried out at room temperature of 293 K. By the use of many investigation techniques, including US velocity and attenuation measurements, DC at 293 K was found to improve by the addition of 10 phr UPE to the blend.

In all the previously quoted investigations, either by low frequency DMTA or by US investigations, the overall compatibility was the main point of interest. Most measurements were carried out at different compositions but at constant temperature. This type of investigation gives information about DC at this temperature. Although some US measurements were done with variation of temperature, the change of dynamic  $T_g$  with composition was the main parameter used to estimate DC. Linear  $T_g$ -composition diagram means perfect compatibility, while deviations from linearity indicate some phase separation. The ultrasonic attenuation measurements have never been used, as much as the author knows, to investigate how does DC vary with temperature.

The aim of the present work is to study the temperature dependence of DC in SBR–NBR blank blends and in blends

*E-mail address:* mohyous1@yahoo.com (M.H. Youssef).

Table 1  
Formulation of specimens

Specimen	SBR (phr)	NBR (phr)	UPE (phr)	Peroxide (phr)
B1	100	0	0	4
B2	75	25	0	4
B3	50	50	0	4
B4	25	75	0	4
B5	0	100	0	4
P1	100	0	10	4
P2	75	25	10	4
P3	50	50	10	4
P4	25	75	10	4
P5	0	100	10	4

containing 10 phr UPE. This is done by measuring the variation of US attenuation coefficient  $\alpha$  with temperature in the region of dynamic glass transition. From the  $\alpha$ - $T$  curves, isothermal compatibility diagrams at different temperatures can be constructed, from which DC can be deduced at any temperature.

## 2. Preparation of specimens and experimental technique

### 2.1. Materials

The materials used in the present study are as follows:

1. The prepared unsaturated polyester (UPE) is based on *p*-carboxy phthalanilic acid and maleic anhydride with ethylene glycol. The final form of UPE is a brown viscous resin with acid number 7.65 mg KOH/g sample. The details of UPE preparation, the rheometric, FTIR, NMR characterization are fully described in a previous work [12].
2. Styrene-butadiene rubber (SBR 1502), styrene content of 23.5%, with specific gravity of  $0.945 \pm 0.005$  and Moony viscosity (ML 4) of about 52 at 373 K.
3. Acrylonitrile-butadiene rubber (NBR) (Krynac 34-52), acrylonitrile content of 33%, with specific gravity of  $0.990 \pm 0.005$  and Moony viscosity (ML 4) of about 45 at 373 K.

Keeping all conditions of mixing the same, the prepared samples were mixed with 4 phr dicumyl peroxide obtained from Aldrich Co. The rubber mixes with and without 10 phr of the prepared UPE were mixed on a two roll laboratory mill of outside diameter 470 mm and working distance

Table 2  
Values of  $T_g$  obtained from DSC

Specimen	B1	B2	B3	B4	B5	P1	P2	P3	P4	P5
$T_g$ (K)	224	228	230	226	251	233	238	228	235	250
		251	251	248				249	251	

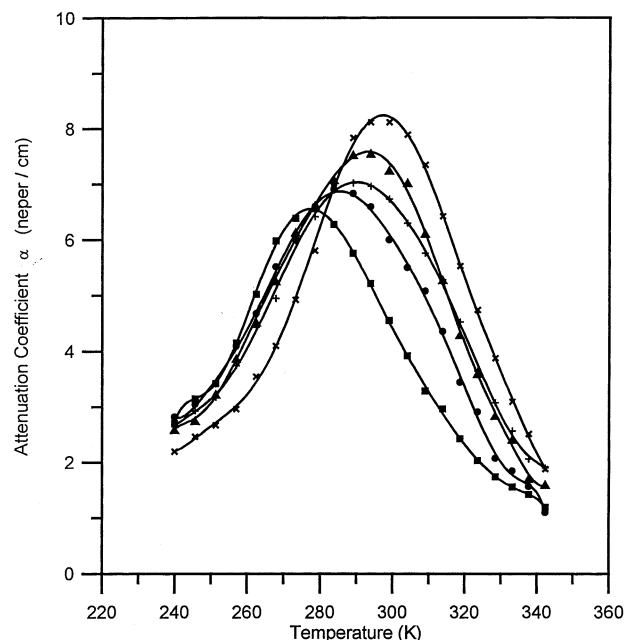


Fig. 1. Variation of US attenuation coefficient with temperature in B1 (■), B2 (●), B3 (+), B4 (▲), B5 (×).

300 mm, speed of slow roll 24 rpm and gear ratio 1:1.4. After complete mixing, the rubber mixes were subjected to sheeting on the mill. The vulcanization was carried out in a heated flat press under a pressure of about 4 MPa ( $40 \text{ kg/cm}^2$  and a temperature of  $415 \pm 1 \text{ K}$ ). Circular disks of thickness 3 mm were obtained. The specimen formulations are given in Table 1. All used solvents and chemical reagents were of pure grade.

### 2.2. Differential scanning calorimetry

Differential scanning calorimeter measurements (DSC) are performed using Shimadzu DSC-50 for accurate determination of glass transition temperatures  $T_g$ . The specimen was fast cooled to 173 K and DSC was recorded on heating up to 373 K at a rate of 5 K/min. The values of  $T_g$  were reproducible within  $\pm 1 \text{ K}$  and are shown in Table 2. Some specimens show single glass transition temperature while others show two glass transitions.

### 2.3. Ultrasonic technique

Ultrasonic measurements were performed using an ultrasonic flaw detector of type Krautkrämer-Branson USD10. The adopted technique is the pulse-echo immersion technique [14]. An US transducer of frequency 5 MHz was bonded to an immersion tank of volume  $4.6 \times 4.4 \times 5.2 \text{ cm}^3$ . The immersion liquid is chosen to be ethyl alcohol. The sample was immersed in the alcohol and were both cooled down to 230 K at a rate of 1 K/min. The measurements were recorded while both alcohol and the immersed sample were heated up to 346 K at the same

Table 3  
Values of peak width  $W$ , peak height  $H$  and their ratio calculated from Fig. 1 for blank SBR, NBR and their blends

Specimen	Peak width $W$ (K)	Peak height $H$ (neper/cm)	$W/H$ (K cm/neper)
B1	38	6.57	5.79
B2	46.5	6.85	6.79
B3	49	7.03	6.97
B4	45.5	7.60	5.98
B5	39.5	8.29	4.76

rate. A useful equation is used to calculate the attenuation [14]:

$$\exp(-2\alpha_r L) = R \exp(-2\alpha_a L) \left[ \left( \frac{\rho_a V_a}{4\rho_r V_r} \right) + \left( \frac{\rho_r V_r}{4\rho_a V_a} \right) + \frac{1}{2} \right] \quad (1)$$

where the subscripts 'a' and 'r' stand for alcohol and rubber, respectively,  $V$  is the ultrasonic velocity,  $L$  is the specimen thickness,  $\alpha$  is the attenuation coefficient,  $\rho$  is the density and  $R$  is the ratio of the received amplitudes when the specimen is immersed and removed and is always less than unity as long as the attenuation in rubber is greater than the attenuation in alcohol which is always true in this study. Since the acoustic impedances ( $\rho V$ ) for rubber and alcohol are close, the last bracket in Eq. (1) is close to unity and the equation reduces to

$$\alpha_r = \alpha_a - (1/2L)\ln R \quad (2)$$

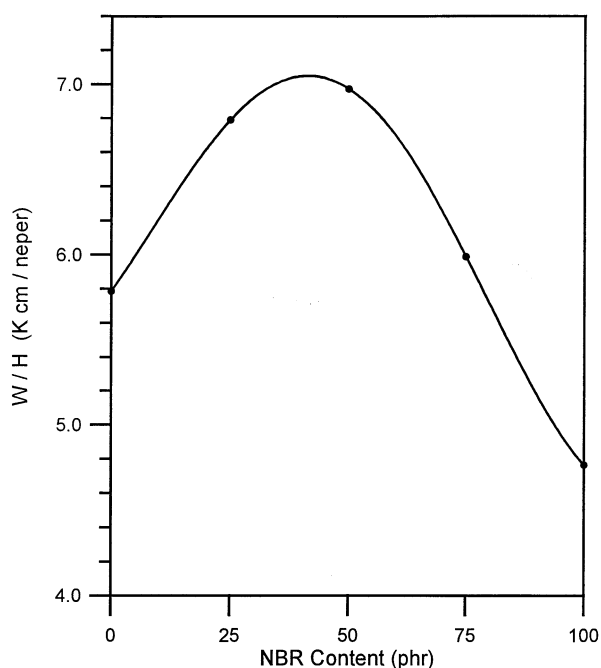


Fig. 2. Variation of peak broadness (ratio of width to height) with NBR content in B-specimens.

The error in measuring the attenuation in rubber does not exceed 5%.

### 3. Experimental results and discussion

#### 3.1. Estimation of compatibility in SBR–NBR blank blends

##### 3.1.1. The overall compatibility

The variation of  $\alpha$  with  $T$  for B1, B2, B3, B4 and B5 is shown in Fig. 1. The exhibited peaks for the individual polymers, B1 and B5, were attributed to the glass–rubber transition [12]. Three evident features can be observed in Fig. 1.

(a) *The peak height* increases with increase of the NBR content in the specimen. The peak height is known to be dependent on the number of relaxing elements in the specimen. In addition to the segmental micro-Brownian motion of the polymer backbone, which exists equally in SBR and NBR during glass–rubber transition, the relaxing dipoles of the acrylonitrile in NBR contribute as well to the relaxation peak [15].

(b) *The peak temperature* shifts to higher values with increase of the NBR content. The polar nature in NBR restricts the segmental motion of the molecule backbone because of the dipole–dipole interaction between neighboring molecules and a long-range cooperative motion is needed to perform the segmental micro-Brownian motion. Thus, higher activation energy is required for the motion of the backbone and thus the transition occurs at temperatures higher than those of pure SBR.

(c) *The peak width* is narrow for unblended polymers B1 and B5 but increases in the blends. Nevertheless, it remains a single peak for each blend. For an incompatible blend, the mechanical loss (and consequently the ultrasonic attenuation coefficient) curves show the presence of two peaks corresponding to the dynamic glass transition temperatures of the individual polymers [3,16,17]. For a highly compatible blend, the curves show only a narrow single peak between the transition temperatures of the individual polymers. An intermediate situation arises when broadening of transition peaks occurs in the case of partially compatible systems, accompanied by a shift in dynamic  $T_g$  to higher or lower temperatures depending on the composition. The broader the transition peak, the more incompatible are the polymers in a blend. The best measure of the broadness of a peak is obtained here by calculating the ratio between the peak width and its height. Table 3 shows values of the peak width ( $W$ ) at  $1/\sqrt{2}$  of its maximum, the peak height ( $H$ ) and as well the ratio ( $W/H$ ) for the blank specimens (B1–B5). The ratio  $W/H$  is plotted against NBR content in Fig. 2. The maximum ( $W/H$ ) value occurs at NBR/SBR content of about 42/58 which is assumed to represent the blend of maximum incompatibility. Fig. 3 shows the variation with

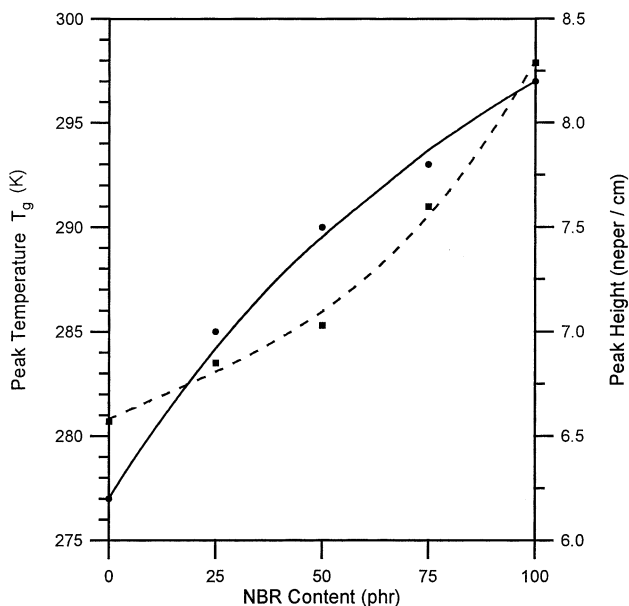


Fig. 3. Variation of peak temperature (●) and peak height (■) with NBR content in B-specimens.

NBR content of the peak temperature and height. The non-linear dependence of the height and temperature of the peak on the NBR content suggests that the two phases are incompatible and some molecular interactions take place between the SBR and NBR blocks.

The glass transition temperature of a polyblend can be calculated from Gordon–Taylor equation [18]:

$$T_{gS} = \frac{w_S T_{gS} + k w_N T_{gN}}{(w_S + k w_N)} \quad (3)$$

where  $w_S$  and  $w_N$  are the weight fractions of SBR and NBR, respectively, while  $T_{gS}$  and  $T_{gN}$  are their corresponding glass transitions.  $k$  is a constant that can be derived from the expansion coefficients of the specimens in their glassy and rubbery states but is usually treated as an arbitrary parameter used to obtain the best fit [19]. If  $k$  is equal to unity the two polymers are compatible and a linear relation is obtained between  $T_g$  and the blend composition. Deviation of  $k$  from unity is taken as a measure of the degree of incompatibility. In Fig. 2 the solid line connecting the  $T_g$  values is the best computer fitting for Eq. (3) obtained with  $k = 1.7$ , which is far from unity. This indicates that SBR and NBR have low overall degree of compatibility, an observation that is supported by the two glass transition temperatures (Table 2) obtained from DSC measurements for B2, B3 and B4.

### 3.1.2. Temperature dependence of compatibility

The previous calculations give an estimate of the overall compatibility of SBR and NBR in a narrow temperature range where the glass–rubber transition takes place in the two components or in their blends. This estimate appears to

be fairly good, but it does not indicate how does the compatibility of the two components change with temperature. The technique adopted here for investigating the temperature dependence of compatibility depends on a model proposed by Takayanagi et al. [20] and modified later by Gary and McCrum [21]. According to this model the logarithmic decrement or the ultrasonic attenuation coefficient of a multi-component system can be written in the form:

$$\alpha = \sum_n w_n \alpha_n \quad (4)$$

where  $w_n$  and  $\alpha_n$  are the weight fraction and ultrasonic attenuation coefficient of the  $n$ th component. In a two-system blend this equation reduces to

$$\alpha = w_S \alpha_S + w_N \alpha_N \quad (5)$$

where the subscripts S and N stand for SBR and NBR, respectively. The values of  $\alpha_S$  and  $\alpha_N$  at different temperatures are taken from the experimental attenuation curves of the individual polymers (B1 and B5). The solid lines in Fig. 4 represent the attenuation coefficient calculated from Eq. (5) for the blends B2, B3 and B4. The fitting curves

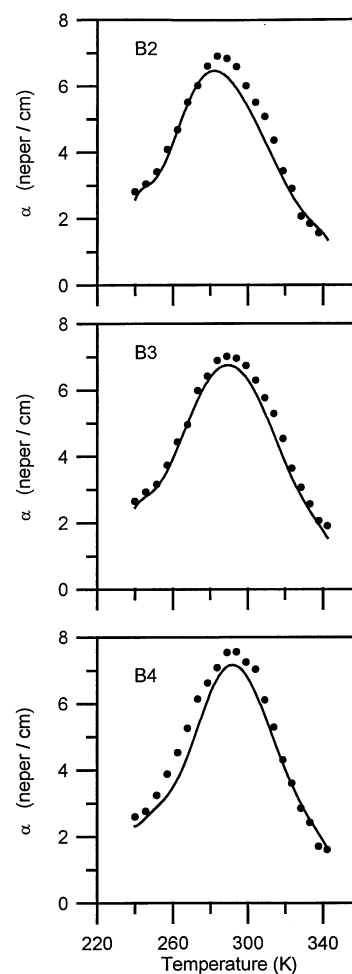


Fig. 4. Variation of US attenuation coefficient with temperature in B2, B3 and B4. The solid line represents the fitting of Eq. (5).

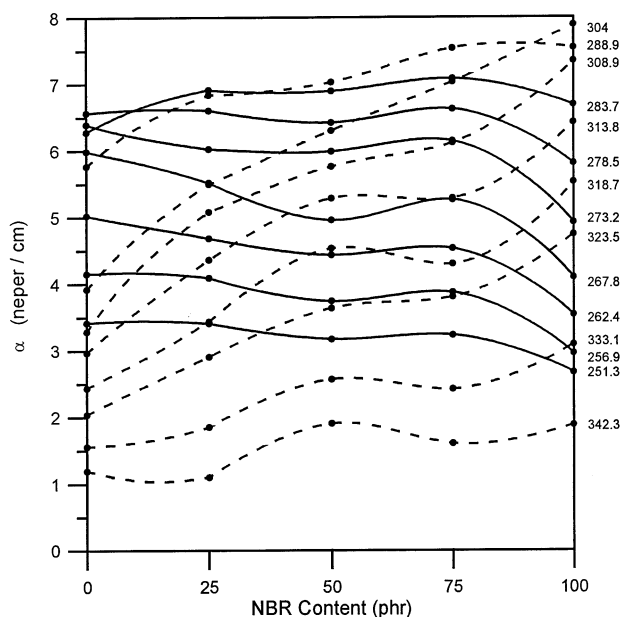


Fig. 5. Isothermal compatibility curves in B-specimens. Variation of US attenuation coefficient with NBR content at certain investigated temperatures (written on the right y axis).

show satisfactory coincidence with experimental points in certain temperature regions but deviate considerably in other regions. This indicates that the compatibility of SBR and NBR in the blends is not perfect at all temperatures. It is evident that the deviation of the fitting from the experimental points appears to be maximum at the peak region where the experimental points have higher values.

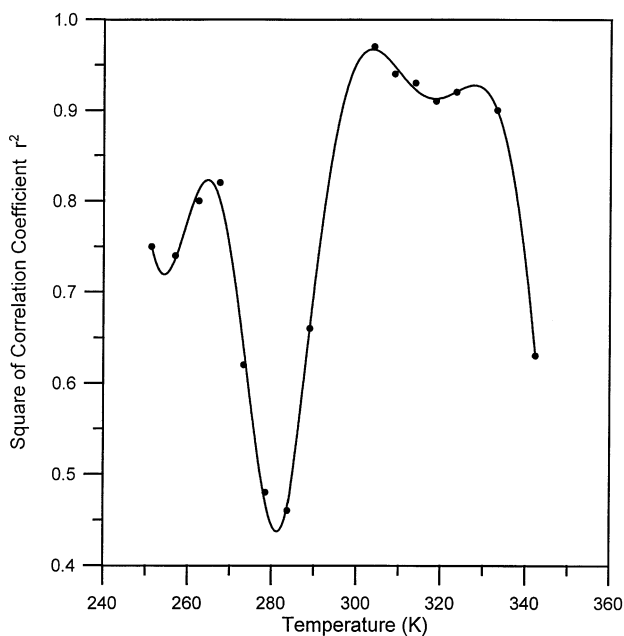


Fig. 6. Variation of square of correlation coefficient  $r^2$  with temperature in B-specimens. The values of  $r^2$  are obtained from the best linear fittings of isothermal curves in Fig. 5.

A more accurate estimate of the variation of compatibility with temperature appears to be a necessity. Fig. 5 shows the variation with NBR content of the attenuation coefficient at certain temperatures, obtained from the experimental points of Fig. 1. To avoid confusion in Fig. 5 some points are connected with dashed lines and others with a solid line. Some these lines approach linearity at certain temperatures, indicating a fairly high compatibility, while others deviate considerably from linearity, indicating high incompatibility. A quantitative estimate can be done by making a least square fitting of points at each temperature (not shown in Fig. 5). The correlation coefficient  $r$  is often used as a statistical quantity that varies between  $-1$  and  $1$  and provides a measure of how data measured between two variables can be closely related to a straight-line regression. For  $N$  data points, the correlation coefficient is defined as [22]:

$$r = \frac{\sum X_i Y_i - (\sum X_i)(\sum Y_i)/N}{\left\{ \left[ \sum X_i^2 - (\sum X_i)^2/N \right] \left[ \sum Y_i^2 - (\sum Y_i)^2/N \right] \right\}^{1/2}} \quad (6)$$

where the summation extends from  $i = 1$  to  $N$ . Since the correlation coefficient has the same sign as the slope of the line, it is preferable to use the square of the correlation coefficient  $r^2$  as a quantitative measure of how experimental points fit well to the linear regression. The higher the  $r^2$  of each fitting, the higher is DC. Fig. 6 shows the variation of  $r^2$  with temperature. The compatibility is moderate at temperatures below 270 K where the two polymers are still in their glassy state. A drastic drop in DC occurs between 270 and 282 K, the region in which SBR passes through its glass–rubber transition. Thus, the compatibility reaches a minimum when SBR is rubbery while NBR is glassy. As NBR starts to approach the glass–rubber transition, the compatibility starts to improve again and reaches relatively high values between 300 and 333 K, a region in which the two polymers are rubbery. Above 333 K DC starts to drop again. This phase separation induced by heating was recorded for many polymeric blends [23] and was attributed to differences, between the two polymers, in the free volume expansion when the blends are heated.

### 3.2. Estimation of compatibility in SBR–NBR blends containing 10 phr of unsaturated polyester

#### 3.2.1. The overall compatibility

Fig. 7 shows the variation of ultrasonic attenuation coefficient with temperature for P1, P2, P3, P4 and P5. There is an increase in the peak height and peak temperature with increase of NBR content. The most pronounced effect associated with addition of UPE is the shift of P1 peak to a temperature higher than that of B1 peak. This is consistent with DSC data which show an increase in  $T_g$  of SBR when UPE is added. Meanwhile, P5 peak suffers almost no shift relative to B5 due to addition of UPE which is again in harmony with the present DSC data and the results of a previous work by the author et al. [12].

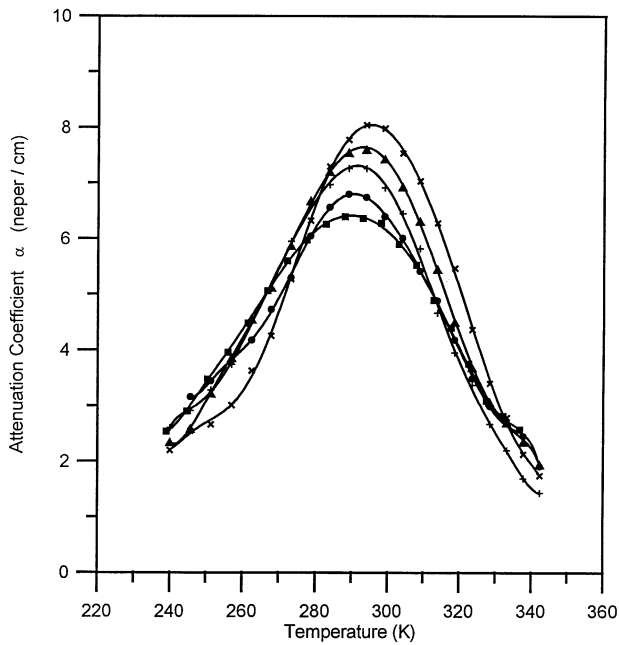


Fig. 7. Variation of US attenuation coefficient with temperature in P1 (■), P2 (●), P3 (+), P4 (▲), P5 (×).

Table 4 shows the peak width ( $W$ ), the peak height ( $H$ ) and the ratio ( $W/H$ ) for the P specimens. Fig. 8 shows the variation of  $W/H$  with NBR content which appears as a monotonic decrease with no peaks. In comparison with Fig. 2, it is quite evident that the addition of UPE increases the broadness of the SBR peak while it has a negligibly small effect on the broadness of the NBR peak. Fig. 9 shows the dependence of the peak temperature and peak height on the NBR content. The experimental points of the peak temperature fit well to the solid line representing Eq. (3) with  $k = 1$ , thus indicating an improved overall compatibility. This improvement is attributed to the increase of  $T_g$  of SBR due to addition of UPE, thus reducing the difference in the glass transition temperature of the two individual polymers.

3.2.2. Temperature dependence of compatibility

The solid line in the three diagrams of Fig. 10 represents the variation with temperature of  $\alpha$ , calculated from Eq. (5), for specimens P2, P3, P4. The values of  $\alpha_S$  and  $\alpha_N$  at

Table 4  
Values of peak width  $W$ , peak height  $H$  and their ratio calculated from Fig. 7 for SBR, NBR and their blends containing 10 phr UPE

Specimen	Peak width $W$ (K)	Peak height $H$ (neper/cm)	$W/H$ (K cm/neper)
P1	52	6.45	8.06
P2	46	6.80	6.77
P3	45	7.32	6.15
P4	45	7.66	5.87
P5	44	8.06	5.46

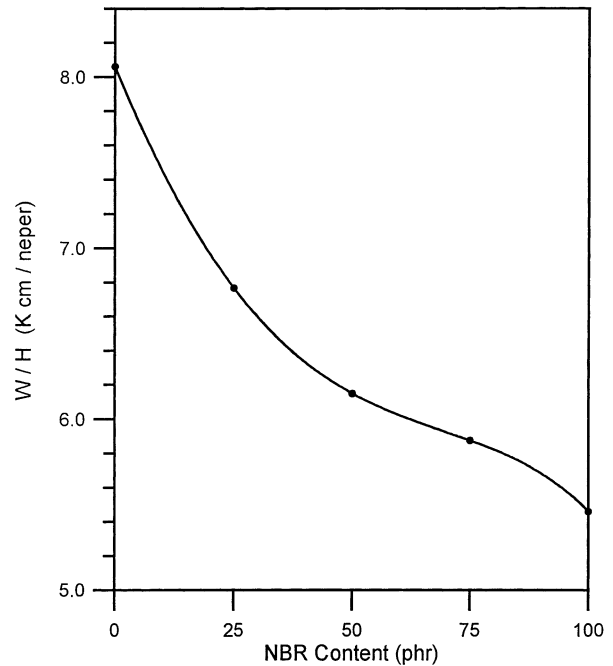


Fig. 8. Variation of peak broadness (ratio of width to height) with NBR content in P-specimens.

different temperatures are taken from the experimental attenuation curves of the individual components (P1 and P5). The coincidence between the calculated values and the experimental data is remarkably improved for P2 after addition of UPE, although some deviations still exist for P3 and P4 in certain temperature ranges. These observations are supported by DSC measurements shown in Table 2. For P2 only one transition appears in the DSC at 238 K.

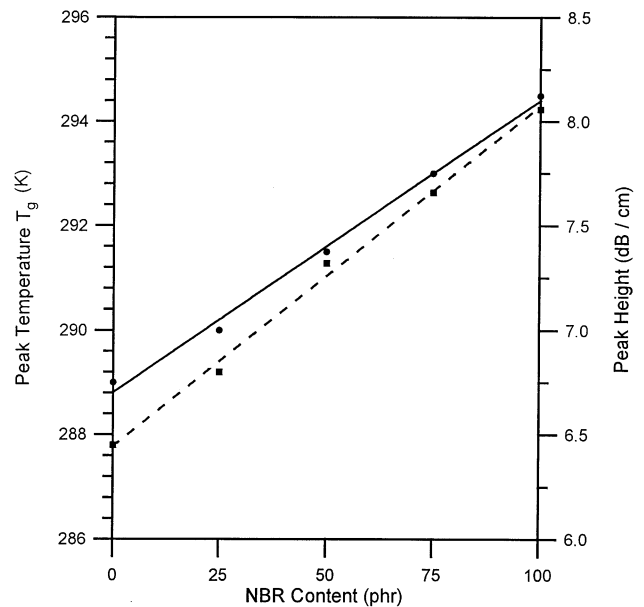


Fig. 9. Variation of peak temperature (●) and peak height (■) with NBR content in P-specimens.

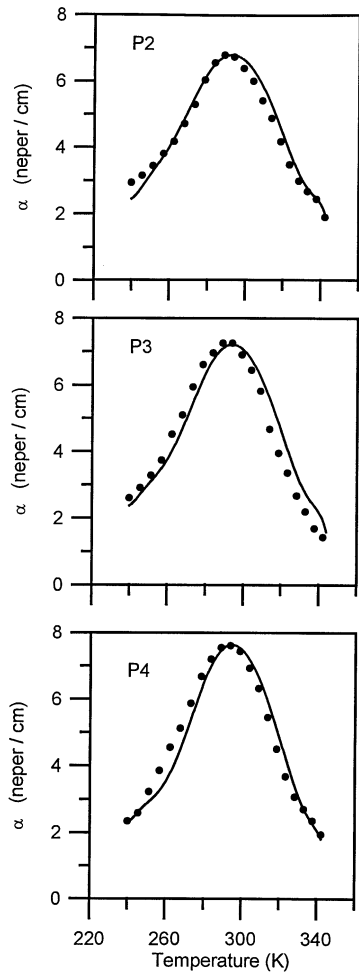


Fig. 10. Variation of US attenuation coefficient with temperature in P2, P3 and P4. The solid line represents the fitting of Eq. (5).

For P3 two transitions appear at 228 and 249 K while for P4 there are two transitions appearing at 235 and 251 K. The appearance of two transitions in DSC measurements indicates a phase separation. Since the fitting of ultrasonic data is perfect only in certain temperature ranges, it is necessary to see how does DC vary with temperature. Fig. 11 shows the variation with NBR content of attenuation coefficient at certain temperatures, obtained from the experimental points of Fig. 7. To investigate how DC change with temperature a least square fitting of points at each temperature is done and the variation of the square of correlation coefficient  $r^2$  with temperature is shown in Fig. 12. Evidently, the addition of UPE improves DC in a certain temperature range (from 288 to 315 K) but becomes worse in other temperature ranges (from 260 to 283 K and above 315 K). Since the previous investigation of compatibility [13], either by ultrasonic velocity and attenuation measurements or dielectric permittivity measurements, were carried out only at room temperature which usually falls between 288 and 315 K, it would be expected that the addition of 10 phr UPE will improve DC at room temperature. On the other hand the blends with UPE

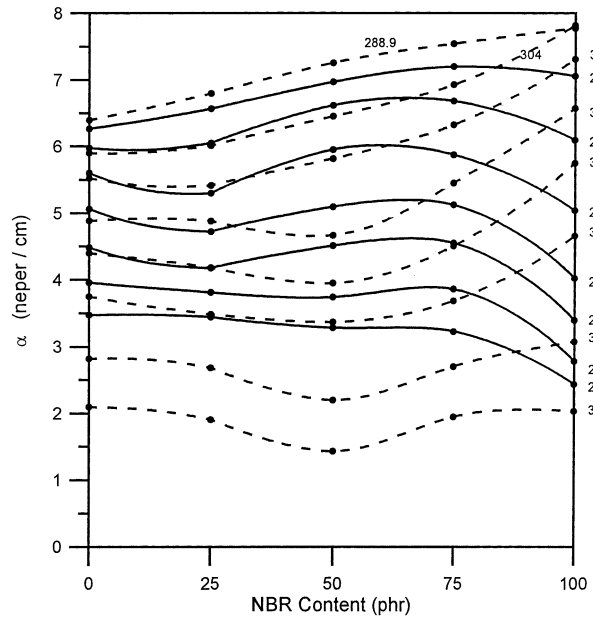


Fig. 11. Isothermal compatibility curves in P-specimens. Variation of US attenuation coefficient with NBR content at certain investigated temperatures (written on the right y axis).

show a sharp drop in DC at temperatures above 333 K, a temperature region in which the blank blends showed moderate degree of compatibility.

#### 4. Conclusion

The variation of ultrasonic attenuation coefficient with

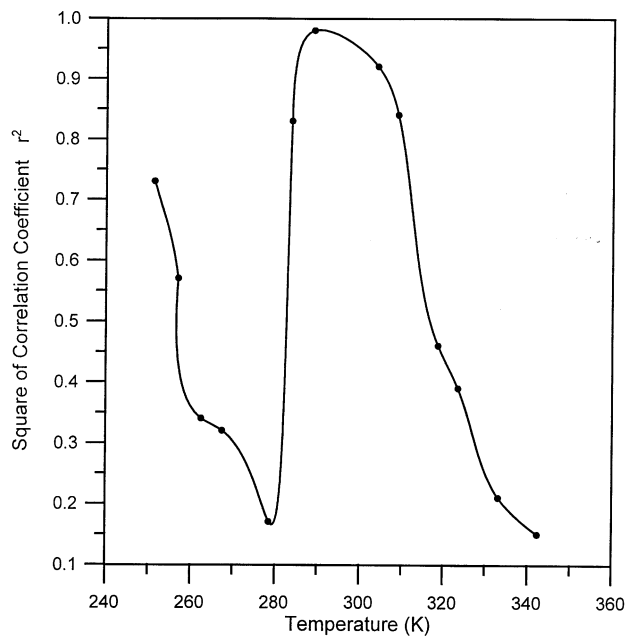


Fig. 12. Variation of square of correlation coefficient  $r^2$  with temperature in P-specimens. The values of  $r^2$  are obtained from the best linear fittings of isothermal curves in Fig. 11.

temperature can be used as a good tool for the investigation of the overall degree of compatibility as well as the dependence of DC on temperature in polymer blends which have close glass transition temperatures. Such an investigation showed that SBR–NBR blends are highly compatible only in a certain temperature range. The effect of addition of 10 phr of unsaturated polyester (UPE) resin showed that the temperature range of high compatibility has changed and that the compatibility diminishes in other temperature ranges. The question of whether the addition of UPE improves DC or not depends strongly on the temperature range at which the blend will be used.

### Acknowledgements

The author wishes to thank Dr S.H. Mansour, Dr S.Y. Tawfik and Prof. Dr A.F. Younan of the Polymer and Pigment Department, National Research Center, for the preparation of UPE and the rubber mixes.

### References

- [1] Poshyachinda S, Edwards HGM, Johnson AF. *Polymer* 1996;37:5171.
- [2] Sierra CA, Galan C, Fatou JG, Parellada MD, Barrio JA. *Polymer* 1997;38:4325.
- [3] Perera MCS. *J Polym Sci, Polym Phys Ed* 1999;37:1141.
- [4] Hourston DJ, Hughes ID. *Polymer* 1978;19:1181.
- [5] Singh YP, Das S, Matti S, Singh RP. *J Pure Appl Ultrason* 1981;3:1.
- [6] Singh YP, Singh RP. *Eur Polym J* 1984;20:201.
- [7] Adachi K, North AM, Pethrick RA, Harrison G, Lamb J. *Polymer* 1982;23:1451.
- [8] Arman J, Lahrouni A, Monge P. *Eur Polym J* 1986;22:955.
- [9] Shaw S, Singh RP. *Eur Polym J* 1987;23:547.
- [10] Sidkey MA, Abd El Fattah AM, Abd El All NS. *J Appl Polym Sci* 1992;46:581.
- [11] Thomas GV, Nair MRG. *J Appl Polym Sci* 1998;69:785.
- [12] Youssef MH, Mansour SH, Tawfik SY. *Polymer* 2000;41:7815.
- [13] Mansour SH, Tawfik SY, Youssef MH. *J Appl Polym Sci* 2001, in press.
- [14] Mason WP, editor. *Physical acoustics, Part A, 1*. London: Academic Press, 1964.
- [15] Cook M, Williams G, Jones TT. *Polymer* 1975;16:835.
- [16] Perepechko I. *Acoustic methods of investigating polymers*. Moscow: Mir Publishers, 1975.
- [17] Manson JA, Sperling LH. *Polymer blends and composites*. New York: Plenum Press, 1976.
- [18] Gordon M, Taylor JS. *J Appl Chem* 1952;2:493.
- [19] Ward IM, Hadley DW. *An introduction to the mechanical properties of solid polymers*. New York: Wiley, 1993.
- [20] Takayanagi M, Harima H, Iwata Y. *Mem Fac Engng, Kyushu Univ* 1963;23:1.
- [21] Gray RW, McCrum NG. *J Polym Sci, Part A-2* 1969;7:1329.
- [22] Mason RL, Gunst RF, Hess JL. *Statistical design and analysis of experiments*. New York: Wiley, 1989.
- [23] Neo MK, Lee SY, Goh SH. *J Appl Polym Sci* 1991;43:1301.